

M.P. Gryaznevich, T.C. Hender, D.F. Howell, C.D. Challis, H.R. Koslowski,
S. Gerasimov, E. Joffrin, Y.Q. Liu, S. Saarelma and JET EFDA contributors

Experimental Studies of Stability and Beta Limit in JET

“This document is intended for publication in the open literature. It is made available on the understanding that it may not be further circulated and extracts or references may not be published prior to publication of the original when applicable, or without the consent of the Publications Officer, EFDA, Culham Science Centre, Abingdon, Oxon, OX14 3DB, UK.”

“Enquiries about Copyright and reproduction should be addressed to the Publications Officer, EFDA, Culham Science Centre, Abingdon, Oxon, OX14 3DB, UK.”

Experimental Studies of Stability and Beta Limit in JET

M.P. Gryaznevich¹, T.C. Hender¹, D.F. Howell¹, C.D. Challis¹, H.R. Koslowski¹,
S. Gerasimov¹, E. Joffrin², Y.Q. Liu¹, S. Saarelma¹ and JET EFDA contributors*

JET-EFDA, Culham Science Centre, OX14 3DB, Abingdon, UK

¹*EURATOM-UKAEA Fusion Association, Culham Science Centre, OX14 3DB, Abingdon, OXON, UK*

²*Association EURATOM-CEA, DSM/DRFC, Cadarache, F-13108, France*

** See annex of M.L. Watkins et al, "Overview of JET Results",
(Proc. 21st IAEA Fusion Energy Conference, Chengdu, China (2006)).*

ABSTRACT.

The paper presents results on the use of the Resonant Field Amplification for experimental probing of stability and β -limits (β is the ratio of the plasma pressure to the magnetic field pressure) in JET. It is found that an externally applied helical magnetic field is strongly enhanced when the plasma exceeds the ideal no-wall stability limit or approaches proximity to other marginally stable (i.e. current-driven) modes. This effect is known as the Resonant Field Amplification (RFA) and was used for the systematic probing of stability in different advanced regimes on JET. The application of this technique on JET is discussed in the paper and the results of the RFA measurements are presented and related to the observed limitations in β .

1. INTRODUCTION.

Advanced tokamak regimes, which are aimed on the steady-state tokamak operation and may significantly increase the power gain in ITER and a fusion reactor, are associated with the increased normalised beta, $\beta_N = \beta_t B_t a / I_p$ ($\beta_t = 2\mu_0 \langle p \rangle / B_t^2$) and are often limited by pressure-driven MHD instabilities. Although the presence of a conducting wall increases this β -limit, it is important to know the ideal no-wall β -limit as Resistive Wall Modes (RWM) can occur above this level. The growth of the RWM strongly depends on plasma rotation profile, current density, pressure profiles, plasma shape, distance of the wall etc. The order of magnitude of these stabilising mechanisms in future devices can be different from one in the present tokamaks, so it is useful to know the ideal limit above which the plasma stability depends on damping and stabilisation.

It has been found that the Resonant Field Amplification (RFA) [1] of an externally applied helical magnetic field is significantly enhanced when a plasma exceeds the ideal no-wall stability limit [2-3], suggesting this might be used as an indication of the no-wall beta limit. The RFA probing has recently been used in scenario development of high-beta discharges on JET [4]. An increase in plasma response to the applied helical $n=1$ field has been also observed before a fast rotating (~ 5 kHz) internal kink or tearing mode was destabilised [5]. It was also found, that enhanced RFA can be observed at lower β , for example, during ELM-free H-mode periods and in particular before the first type-I ELM.

In this paper we present results of the RFA measurements in high- β scenarios in JET. The experimental set-up, the hardware and the description of the methods used for data analysis are presented in the Section 2. In Section 3 we discuss the complication of the no-wall limit identification from the RFA connected with ELMs and other modes. In Section 4 we present initial results of the RFA measurements in advanced regimes on JET. Section 5 gives the conclusions.

2. THE EXPERIMENTAL SET-UP AND METHODS OF THE NO-WALL LIMIT IDENTIFICATION.

Resonant Field Amplification was studied on JET in three advanced regimes: the hybrid regime, with low magnetic shear and $q(0)$ close to 1 [6], and high-beta plasmas being developed for steady-

state application, with low or reversed magnetic shear and $1.0 < q_{\min} < 2.5$, including regimes with [7] and without [8] Internal Transport Barriers (ITBs). Hereafter, these plasma classes will be referred to as ‘hybrid’, ‘high- β low shear no-ITB’ and ‘high- β with ITB’ regimes, respectively. These studies were carried out by measuring the plasma response to an applied AC $n=1$ or $n=2$ helical magnetic fields produced by the JET external Error Field Correction Coils (EFCC) [9], Fig.1. Here time dependencies are shown of the plasma current, I_p , total Neutral Beam (NB) power, normalised beta, β_N , amplitudes of $n=1$ (red) and $n=2$ (blue) modes (arbitrary values), EFCC current and the plasma response component of B_r , which is an $n = 1$ combination of midplane saddle loops signals in octants orthogonal to the applied perturbation and proportional to the RFA. We define the RFA as a ratio of the plasma response to the applied field,

$$\text{RFA}(r, \phi) = (B_r(r, \phi) - B_{r,\text{vac}}(r, \phi))/B_{r,\text{vac}}(r, \phi) \quad (1)$$

and the explanation of how we are measuring the plasma response is given below.

The measured plasma response to a non-perturbative low-level $n = 1$ stationary AC field shows a pronounced increase in all three advanced regimes, as seen in the time evolution of the plasma response component of the B_r . In these experiments, four external Error Field Correction Coils, Fig.2, were powered from two independent power supplies allowing application of a stationary or rotating $n=1$ magnetic field. To measure the RFA, EFCC currents of 200– 800A ($\times 16$ turns) have been used with frequency from 3Hz to as high as 60 Hz. The higher frequency was used to increase the time resolution for the plasma response measurements during fast increase in β in some regimes and also to study plasma response during ELM-free periods and in proximity of $n=1$ modes. Either pair of EFCCs in Octants 1 – 5 or 3 – 7 was used to produce an $n = 1$ field and the plasma response was measured with combination of midplane in-vessel saddle loops in Octants 1, 3, 5 and 7. When the $n = 1$ travelling waves with frequencies from ± 3 Hz to ± 20 Hz have been applied by using both pairs of EFCCs with currents shifted in time by a half period, the measured plasma response shows a distinct maximum at $f \sim +3 - +5$ Hz (positive corresponds to rotation in the ion drift direction) and results were compared with an analytic model and MARS-F simulations [10] showing qualitative agreement. Experimental results from DIII-D and a simple single-mode model [3] suggest that the maximum amplification is observed when the externally applied field rotates with a frequency of a fraction of the inverse wall time corresponding to the natural rotation frequency of the stable RWM. If we expect that the measured RFA is connected with the RWM, the plasma response should significantly reduce with the increased frequency of the applied field. However, in our experiments when standing waves have been applied using only one of EFCCs pairs, a good signal-to-noise ratio of the plasma response could still be measured with EFCC current frequency up to 60Hz, although it was necessary to increase the current in the EFCCs from typically used 400-500A at 5-30Hz to 600-800A at 60Hz.

The perturbation induced by the EFCCs was typically > 5 times below the the level of the error field or externally applied helical field that cause locked mode in studied regimes, and was not seen

by any other (but magnetic) diagnostics. Usually, for the $n = 1$ RFA measurements, only one pair of EFCCs has been used. JET has saddle loops situated in an octant orthogonal to the octants of the used EFCCs which will not detect any vacuum field if connected to measure the $n = 1$ component. In the simplified method of the plasma response measurements, which has been mainly used in this paper, it was measured as a ratio of the total radial field at the vessel measured with a combination of these saddle loops to the total radial field measured by the loops at the EFCCs position. This makes the plasma response measurements much easier if we are not interested in the precise absolute values as only signals from loops in the orthogonal octants need be used. However, at high β_N , the phase shift of the plasma response becomes significant and should be taken into account when absolute values of the RFA are needed (see formula 1). It was difficult to calculate the vacuum field due to a complicated shape of EFCC coils and also due to the presence of a near-by metal structures (e.g. iron core limbs, see Fig.2) and image currents in conducting structures in dynamic regimes, so measurements of the vacuum field at different frequencies have been done in pulses without plasma and were used as a reference. The signal of the plasma response measured by subtraction of the vacuum field required good signal-to-noise quality of both magnetic field and EFCC current measurements and magnetic diagnostics improvements have been taken to achieve these. Mainly this method has been used in the previous studies [11].

Although an increase in the RFA of up to 10 times has been often observed at high β_N and low EFCC frequencies, the absolute value of the measured response did not typically exceeded 5–8% of the applied external helical field, which was $\sim 10^{-3}-10^{-4}$ of the total radial field at the resonant surface $q = 2$. To measure the weak plasma response at β_N close or below the no-wall limit, a sophisticated technique of the synchronous detection was used. The use of synchronous detection was also needed as at higher frequency the probing signal has significant deviation from a pure sine wave. The Fourier analysis of the measured saddle loop signals has been performed and the ratio of amplitudes (at the probing frequency) of the $n=1$ combination of signals measured by saddle loops situated in an octant orthogonal to the octants of the used EFCCs to those at the EFCCs position has been taken as the RFA.

After the RFA signal has been obtained, an averaging has been done over several cycles, typically 3 – 10. The time resolution has also been varied (EFCC frequency) which resulted in a two-parameter smoothing: the number of cycles for averaging and the separate smoothing. The averaging was necessary to reduce the noise and to smooth fast variations in the RFA due to MHD events (this will be discussed in Section 3). However, during fast changes in beta this averaging was not effective and the only way to obtain good data was to increase the frequency of the EFCC current. As was mentioned above, the RFA reduces with increase in the frequency from the maximum value at $f \sim 3-5\text{Hz}$, so the signal-to-noise level reduced at higher f and the analysis was always a compromise between the frequency, time resolution used in analysis and the number of cycles for smoothing. We always compared data obtained with different settings to avoid errors connected with the noise. The optimum frequency for probing was found to be 20 – 40Hz.

The growth of the plasma response has been theoretically predicted by MARS-F code to appear well below the no-wall limit, $\sim 20\%$ for a particular JET equilibrium for a high- β low shear regime pulse with $q_{\min} \sim 1.5$ [11,12], Fig.3. (other cases where the RFA threshold appears at much lower β_N are described below). Fig.4 presents the dependence of the measured $n=1$ RFA on β_N in three pulses in Fig.1, showing a pronounced increase in the RFA (the RFA threshold). Here (and everywhere later in this paper) the RFA is determined as a ratio of signals from combinations of orthogonal saddle loops, from Octants 1-5 and Octants 3-7 (EFCCs in Octants 3-7 were used in this case), which is close to the total $\text{RFA} = (B_r - B_r^{\text{vac}})/B_r^{\text{vac}}$ at β_N values below or close to the no-wall limit. For this type of equilibrium where global modes dominate in the simulations, typically the observed RFA increases linearly with β_N until the threshold is reached, when it will suddenly increase by factor 2–5, as clearly seen in Fig.4. The difference in β between measured RFA limit and calculated no-wall limit for a global pressure-driven kink mode depends on the details of the q and pressure profiles, plasma shape and other parameters.

3. PLASMA RESPONSE IN PROXIMITY OF ELM AND N=1 FAST ROTATING MODE.

A precise understanding of the meaning of the RFA threshold measurements is complicated in the presence of MHD activity or in a case of other (e.g. current-driven) modes being in proximity to unstable conditions. In this case increase in the RFA could be observed even well below the no-wall β -limit determined by the RWM, as predicted by the theory [13].

Figure 5 shows that the behaviour of the $n=1$ RFA does not increase monotonically with β_N with a clear increase in the plasma response during the ELM-free period prior to the first ELM and correlation of a maximum in the RFA with the first type-1 ELM, in high- β low shear no-ITB pulse (left plot) and increase in RFA at low β_N during ELM-free period (right plot). In example shown in the left plot, this increase at $t = 4$ sec happens well below the second increase in the RFA at $\beta_N \sim 2.9$. This is more clearly seen in Fig.6, where RFA for this pulse is plotted versus β_N . The amplification prior to the first ELM in this case started at low β_N value ~ 1 . Although β_N increases at the same time, the increase in the amplification is unlikely to be connected with the change in the β -value and is connected more likely with the development of the edge current density during the ELM-free period that destabilises the edge peeling mode. Fig.5, right plot, shows pronounced increase in RFA at nearly constant β_N . We should remind that the plasma response is measured outside the plasma and hence only a proxy for the RFA, so the comparison of the absolute values of the response to ELMs which comes from the edge to that connected with the RWM that comes from the core can be only quantitative.

A significant increase in the plasma response to the applied external $n=1$ field has been observed prior to the onset of fast rotating $n=1$ modes (typical mode frequency ~ 5 -10kHz), with the increase starting up to 400ms before the mode onset. Fig.7 shows an example of such phenomenon in the high- β pulse with ITB 70069. The EFCC frequency in this pulse was 20Hz. The plasma response reaches its maximum just before the start of the mode at $t = 6.65$ sec. As the β_N value slowly decreases during the amplification rise and fall, the amplification can not be attributed to

this change. In an absence of any other MHD activity at $t < 6.65\text{sec}$ it is difficult to suggest any significant changes in the q -profile, or pressure profile apart of a slow evolution. Further investigation is needed to explain this amplification in the proximity of a fast rotating mode which starts as a kink-mode and then shows resistive (tearing island) structure [5].

4. INITIAL RESULTS OF THE RFA STUDIES IN ADVANCED REGIMES ON JET

More than 150 high- β_N pulses have been analysed using the RFA. In the high- β low or slightly reversed shear plasmas without or with a weak ITB, the time of the neutral beam injection was varied in order to achieve different values of the central or minimum target q -values. A very different behaviour of the RFA is found in these plasmas. The dependence of the $\beta_N^{\text{RFA threshold}}$ on the central or minimal q determined from the EFIT reconstruction constrained by the Motional Stark Effect diagnostics, Alfvén Cascades and low- n MHD is shown in Fig.8, suggesting significant increase of the RFA threshold at lower q_{min} . It was also shown, that the RFA threshold does not vary with internal inductance l_i in the same way as commonly observed for the β -limit showing that there are other effects involved, probably details of the current profile. This is demonstrated in Fig.9, where evolution of the RFA with β_N/l_i in three high- β low or slightly reversed shear pulses with different NBI start time and current ramp-up speed is shown. The RFA threshold varies from $2.4l_i$ at high target q_{min} , early time of the neutral beam injection, to $4.4l_i$ at low target q_{min} , late NBI.

The RFA threshold could be identified both during the beta rise and the beta fall caused by the MHD activity or by the end of the heating phase. Fig.10 shows evolution of the RFA with β_N during β -rise and β -fall periods in the ITB pulse 70069. The threshold is approximately the same in both phases. High β_N could be sustained at $\beta_N \sim 1.2\beta_N^{\text{RFA threshold}}$ for up to 7 seconds, of the order of the characteristic time of the current diffusion [4]. In the high- β low shear no-ITB pulses plasma with $\beta_N \sim 70\%$ above the RFA threshold can be transiently obtained. Fig.11 presents the RFA threshold and the maximum achieved β_N for pulses with different scenarios of the NB heating showing little variation between pulses. This indicates similar good stability properties of these plasmas with achieved β_N well above the RFA threshold.

To understand the observed big gap between the measured RWM threshold and the achieved maximum β_N and the q -dependence of the measured threshold, numerical simulations of the no-wall limit have been performed with linear ideal MHD stability codes MISHKA-1 [14] and MARS-F (including kinetic effects) [10] using experimental equilibrium for typical high- β regimes on JET. The MARS-F simulations have shown that the RFA threshold for JET pulses with different target q_{min} decreases with increasing q_{min} , in the qualitative agreement with the experimental results. The simulations also confirm the existence of the plasma response (amplification) at β -values below the no-wall limit, caused by current-driven modes at lower β -values (MARS-F), and underline the dependence of the RFA threshold on the presence of marginally stable current-driven modes (MARS-F, MISHKA-1). These results may help to explain the non-monotonic behaviour of the measured RFA which has been observed in some cases (see Fig.4).

CONCLUSIONS.

Extensive use of the Resonant Field Amplification (RFA) measurements as a routine diagnostic on JET shows that it can be used for stability probing of a tokamak plasma, sensitive to both pressure and current density profile. It has been shown that the RFA threshold on JET decreases with increasing q_{\min} , as was predicted by the modelling. This new diagnostic also allows estimation of the duration of the plasma sustainment over the RFA threshold. Values of β_N up to 70% above the measured RFA threshold have been transiently obtained on JET.

ACKNOWLEDGEMENTS.

The authors would like to thank L Moreira, D Rendall, S Hotchin and M Bigi for providing technical support to the EFCC power supplies use and EFCC operations. This work was funded by the UK Engineering and Physical Sciences Research Council and by the European Communities under the contract of Association between EURATOM and UKAEA. The views and opinions expressed herein do not necessarily reflect those of the European Commission. The work was undertaken under the European Fusion Development Agreement.

REFERENCES

- [1]. Boozer A.H. 2001 *Physical Review Letters* **86**, 5059
- [2]. Garofalo A, et al 2002 *Physic Plasmas* **9** 1997
- [3]. Reimerdes H, et al., 2004 *Physical Review Letters* **93**, 135002
- [4]. Gryaznevich M P *et al* 2007 Experimental identification of the beta limit in JET *Proc. 34th EPS Conference on Controlled Fusion and Plasma Physics (Warsaw, 2007)* P1-070
- [5]. Buratti P, 2008 *to be published in Proceedings of 35th EPS Conference on Plasma Physics, Crete, 2008*, P1-069
- [6]. Joffrin E, et al., 2004 *Nuclear Fusion* **45** 626
- [7]. Challis C.D. *et al* 2007 High β_N JET H-modes for steady-state application *Proc. 34th EPS Conference on Controlled Fusion and Plasma Physics (Warsaw, 2007)* P5-124
- [8]. Mailloux J. *et al* 2007 Development of ITB plasmas at high β_N and high triangularity in JET *Proc. 34th EPS Conference on Controlled Fusion and Plasma Physics (Warsaw, 2007)* P4-151
- [9]. Barlow I, et al., 2001 *Fusion Eng. Des.* **58–59** 189
- [10]. Liu Y.Q, et al., *Phys. Plasmas* **13**, 056120 (2006)
- [11]. Gryaznevich M.P, et al, 2003 *Bull. Am. Phys. Soc.* **48** RP1.036
- [12]. Hender T.C, et al., 2004 *in Fusion Energy 2004 (Proc. 20st International Conference Villamoura, Portugal, 2004)*, (Vienna: IAEA) CD-ROM file EX/P2-22 and <http://www-naweb.iaea.org/napc/physics/FEC/FEC2004/datasets/index.html>
- [13]. Pustovitov V.D. 2003 *JETP Lett.* **78** 281
- [14]. Mikhailovskii A.B. et al., 1997 *Plasma Physics Reports* **23** 884

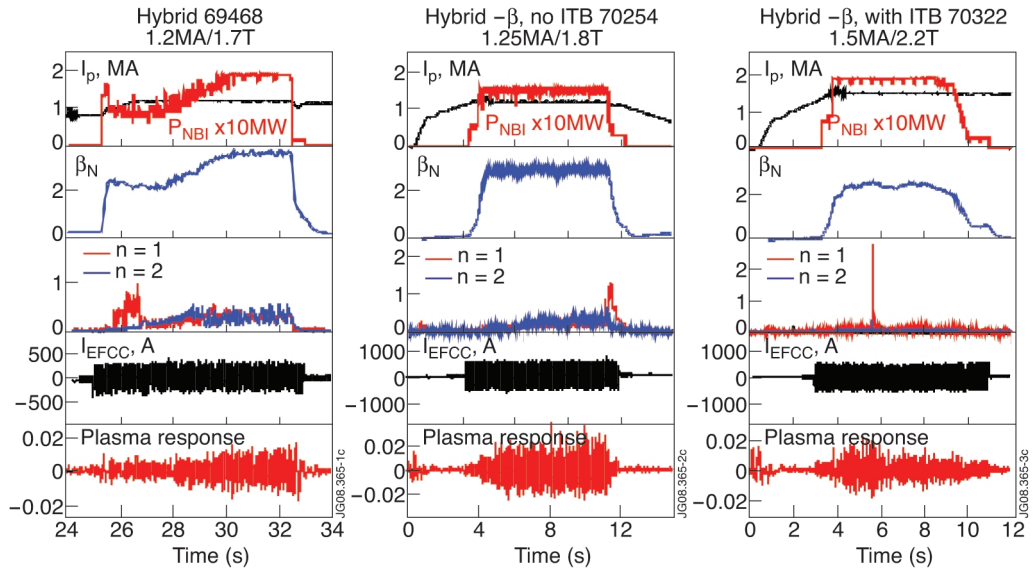


Figure 1: RFA in different JET scenarios: (a) hybrid low-shear regime, Pulse No: 69468, (b) high- β_N low or slightly reversed shear (no or weak ITB) regime, Pulse No: 70254; (c) reversed shear high β_N regime with ITB, Pulse No: 70322.

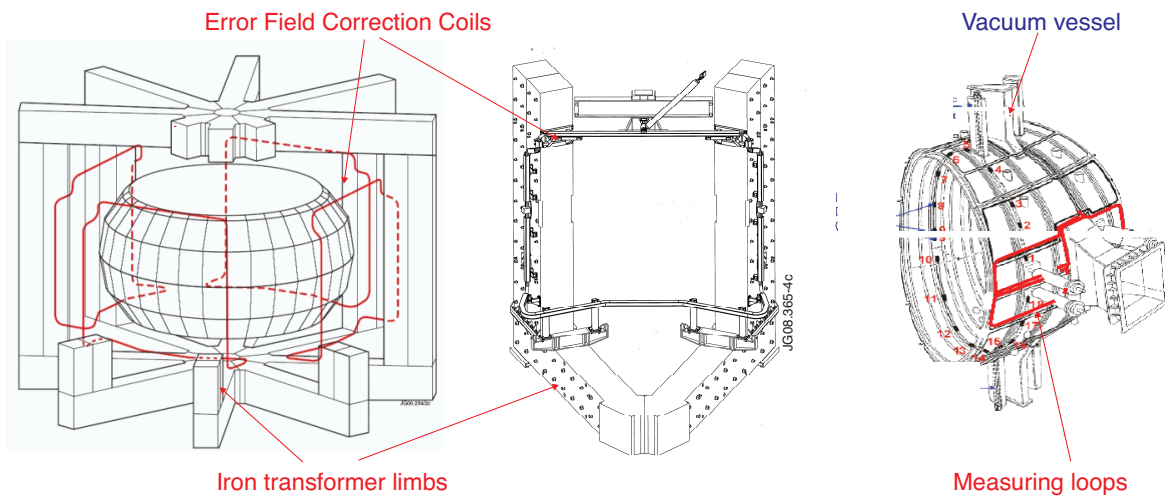


Figure 2: Position of the external Error Field Correction Coils and measuring loops. The middle picture shows one of eight octants and EFCC coil is situated between limbs of the iron transformer and the mechanical support structure of the vacuum vessel.

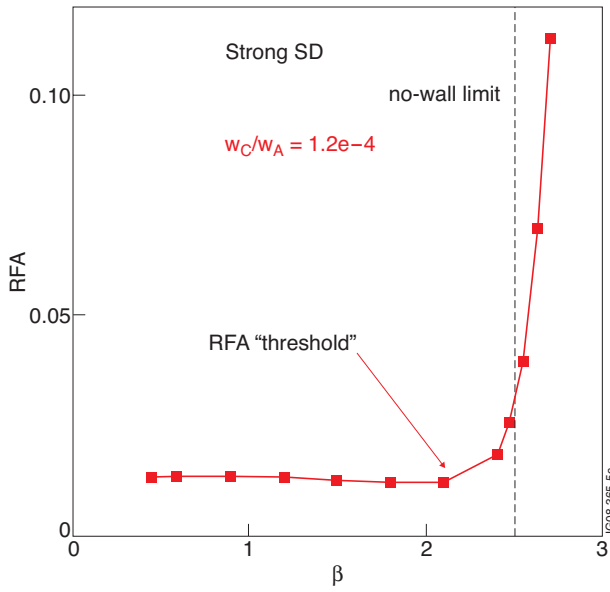


Figure 3: The predicted (MARS-F) dependence of the $n=1$ RFA on β_N in a typical high- β JET pulse.

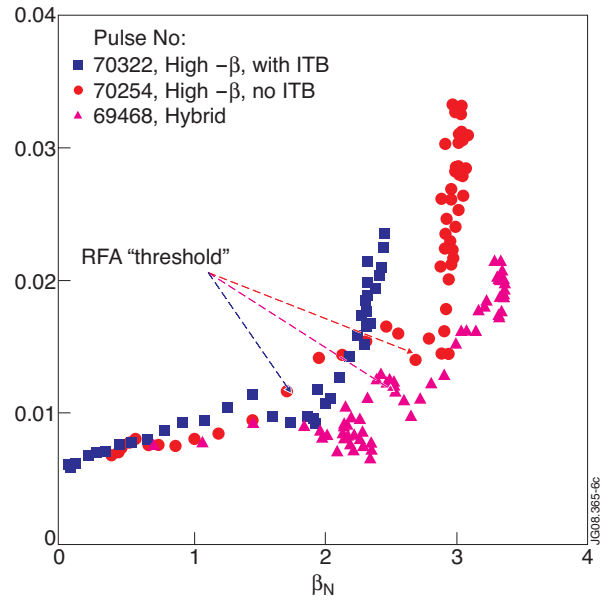


Figure 4: The dependence of the $n=1$ RFA on β_N in three high- β_N pulses shown in Fig.1.

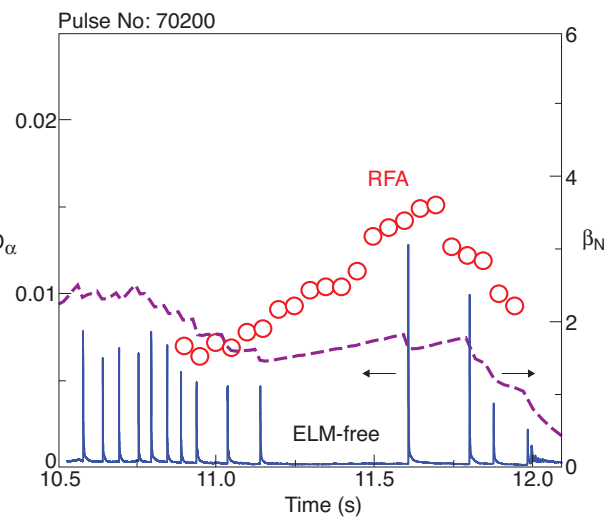
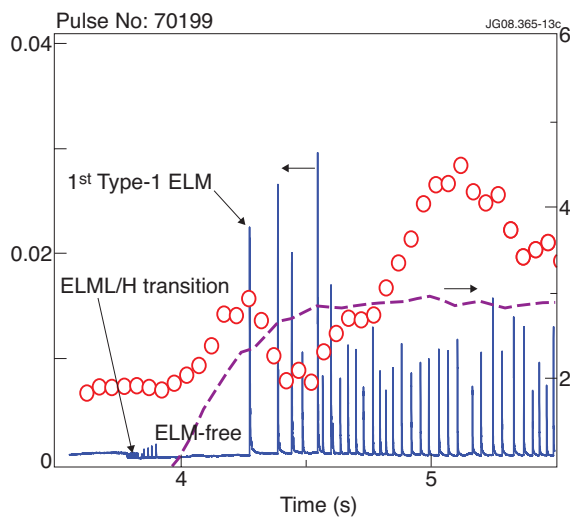


Figure 5: $n=1$ RFA (red circles), D_α (blue) and β_N (magenta) in two high- β -no-ITB pulses.

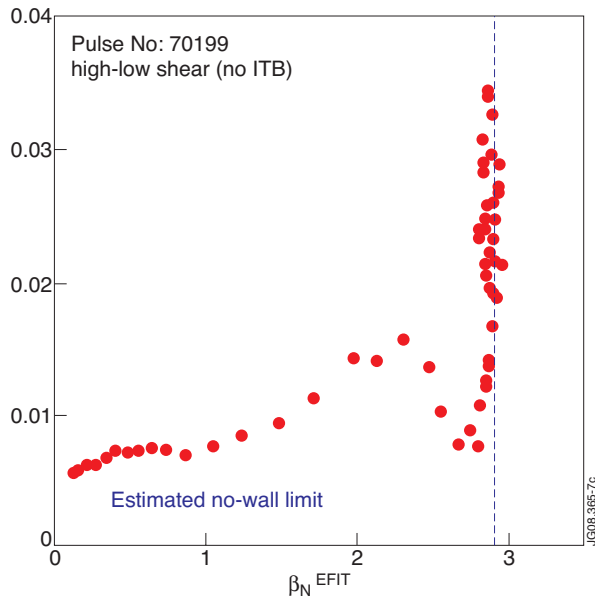


Figure 6: Increase in RFA below no-wall limit in high- β_N low shear pulse.

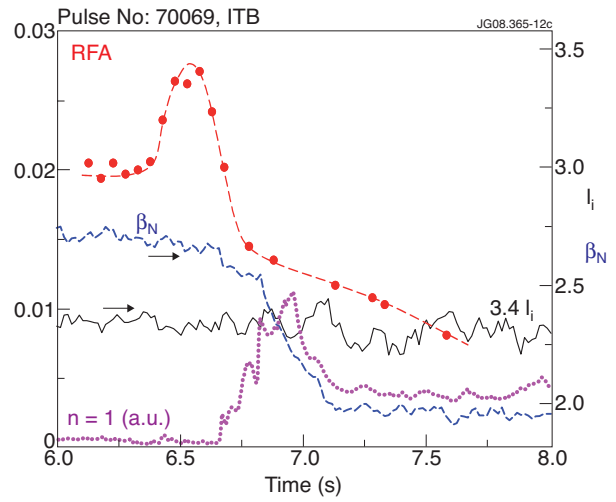


Figure 7: RFA (red), β_N (blue), $3.4 I_i$ (black) and $n=1$ 5kHz mode amplitude (magenta) in a high- β_N ITB Pulse No: 70069.

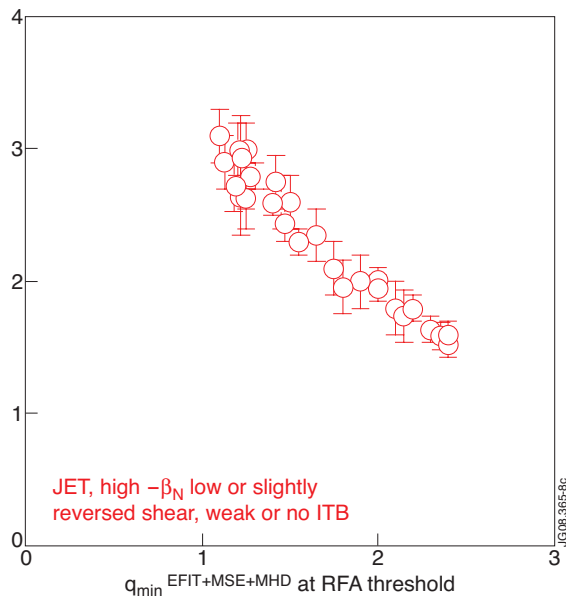


Figure 8: RFA threshold measured in the high- β_N low or slightly reversed shear pulses at different target q_{min} .

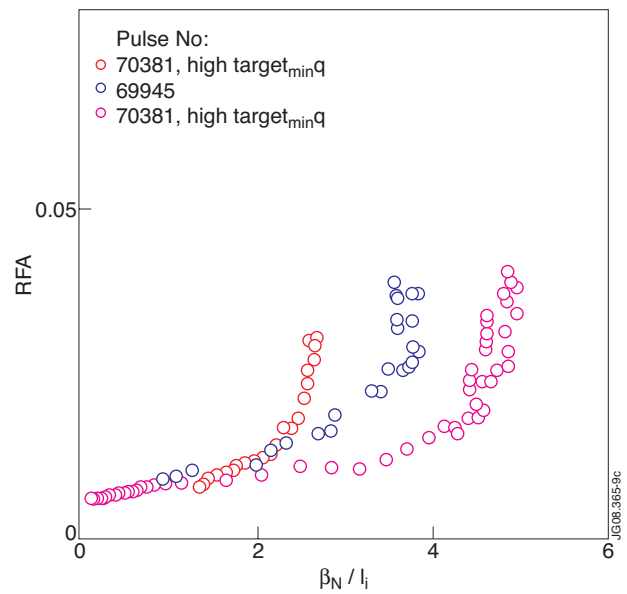


Figure 9: RFA dependence on β_N / I_i in three high- β_N low or slightly reversed shear pulses at different target q_{min} .

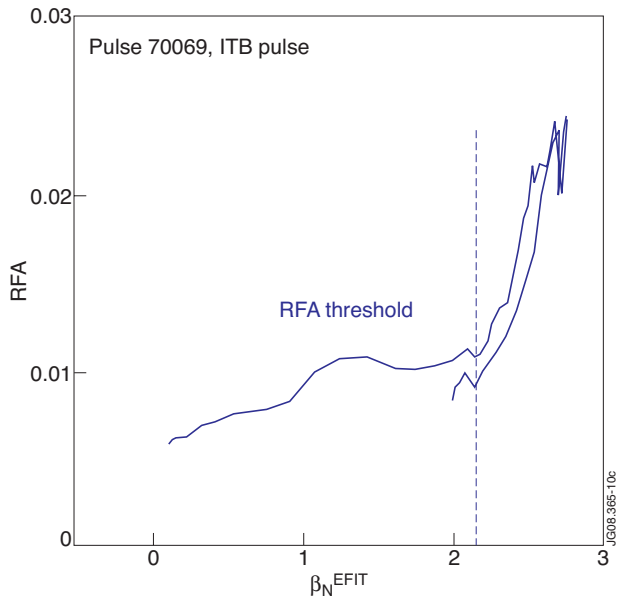


Figure 10: RFA threshold measured in the high- β_N ITB Pulse No: 70069 during beta ramp-up and ramp-down phases.

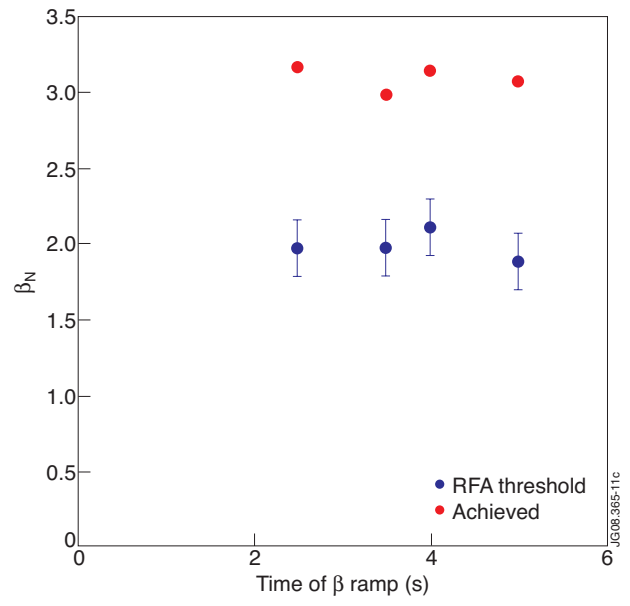


Figure 11: RFA threshold and the maximum achieved β_N in high- β low shear no-ITB pulses with different time of the NB heating.